Kora *Bioresour. Bioprocess.* (2018) 5:30
https://doi.org/10.1186/s40643-018-0217-5

Bioresources and Bioprocessing

RESEARCH Open Access

Bacillus cereus, selenite-reducing bacterium from contaminated lake of an industrial area: a renewable nanofactory for the synthesis of selenium nanoparticles

Aruna Jyothi Kora*

Abstract

Background: An attempt was made to isolate selenite-reducing bacteria from a contaminated lake that receives industrial effluents and domestic sewage. The isolated dominant bacterial strain *AJK3* was identified as *Bacillus cereus*, based on biochemical characterization and 16S rDNA sequencing. The time dependent selenium removal at different selenite concentrations monitored with ICP-AES indicates the substantial selenite reduction capability of the isolated strain. The selenium nanoparticles produced during the bacterial reduction of selenite were analyzed with UV–visible spectroscopy, X-ray diffraction, transmission electron microscopy, zeta potential measurement, Fourier transform infrared spectroscopy and Raman spectroscopy.

Results: The nanoparticle synthesis was confirmed from the red colour emergence in culture broth and wide UV–vis peaks. The produced nanoparticles were polydisperse, spherical, size varied from 50 to 150 nm and the mean particle size was about 93 nm. The amorphous nature of the generated nanoparticles was confirmed from the Raman spectroscopy, XRD and SAED patterns. The IR data and zeta potential values substantiated the protein capping of the produced nanoparticles.

Conclusions: Thus, the present study suggests that the isolated bacterial strain can be exploited as a prospective, renewable, natural, nanofactory for the bacteriogenic synthesis of nanoparticles. Also, the study has application in bioremediation of selenite from the contaminated environment.

Keywords: *Bacillus cereus*, Bacterial reduction, Bacteriogenic, Selenite, Selenium nanoparticles

Background

Various anthropogenic activities are causing disturbances to many ecological systems leading to serious ecological imbalance. This is mainly resulting from the contamination of the environment with toxic heavy metals and metalloids. The microbes surviving in the contaminated sites naturally adapt themselves and such habitats act as potential reservoirs for the competent microorganisms (Ghosh et al. 2008). Bacteria which are exposed to metals and metalloid pollutants in the environment demonstrate a significant resistance towards metal stress by different mechanisms (Dhanjal and Cameotra 2010). Selenium, a metalloid stands at a special position by being an essential trace nutrient at low levels and a toxin at higher concentrations both for the humans and animals. The major sources for the toxic species of selenium: selenate (Se^{6+}), selenite (Se^{4+}), and selenide (Se^{2-}) are industrial effluents, sewage sludges, and agricultural drainage (Ghosh et al. 2008; Husen and Siddiqi 2014). The bacterial reduction of selenium oxyanions such as selenite to elemental selenium is one of the major biogeochemical processes involved in

*Correspondence: koramaganti@gmail.com
National Centre for Compositional Characterisation of Materials (NCCCM), Bhabha Atomic Research Centre (BARC), ECIL PO, Hyderabad 500 062, India

selenium removal from the agricultural drainage water and sediments. Thus, the bacteria play a key role in the biogeochemical cycling of selenium (Bajaj et al. 2012).

Selenite-reducing bacteria have been isolated from a variety of environments including Mono Lake of California (Oremland et al. 2004), Dead sea, a salt lake (Oremland et al. 2004), Caspian sea of Iran (Shakibaie et al. 2015), sediments of Cama-rones river from Atacama desert, Northern Chile (Torres et al. 2012), activated sludge (Srivastava and Mukhopadhyay 2013), sludge of Taiyuan sewage plant, China (Li et al. 2014), drainage slough from Nevada (Oremland et al. 2004), and anaerobic granules from paper mill wastewater treating reactor (Jain et al. 2015). In addition, from the soil of a antimony mine from Lengshuijiang, southern China (Zheng et al. 2014), soil of a magnesite mine from Salem, India (Ramya et al. 2015), soil of a coal mine from West Bengal, India (Dhanjal and Cameotra 2010), selenium laden agricultural soil of North-East Punjab, India (Bajaj et al. 2012), soil of mangrove forest from Bhitarkanika, Orissa, India (Mishra et al. 2011), rhizosphere soil of a selenium hyperaccumulator legume grown in seleniferous mine from Sardina, Italy (Lampis et al. 2014), rhizosphere of wheat grown in herbicide contaminated soil (Dwivedi et al. 2013), and rhizosphere of cereal plants grown in ash-derived volcanic soil of southern Chile (Durán et al. 2015). Others include rock fragments of black oil shale from Haenam, Korea (Tam et al. 2010), food wastes collected from local market of Giza, Egypt (Khiralla and El-Deeb 2015), sub gingival dental plaque (Pearce et al. 2008) etc. Thus, a large number of selenite-reducing bacteria have been known to produce selenium nanoparticles under both aerobic and anaerobic conditions (Husen and Siddiqi 2014).

The selenium nanoparticles are bestowed with multifaceted biological properties mainly due its high bioavailability and biocompatibility; and low cytotoxicity (Shakibaie et al. 2010; Wang et al. 2010, 2013). A wide variety of properties shown by selenium nanoparticles are free radical scavenging (Huang et al. 2003), antioxidant (Forootanfar et al. 2014; Kong et al. 2014; Mittal et al. 2014; Ramya et al. 2015; Rezvanfar et al. 2013; Torres et al. 2012; Wang et al. 2013), chemoprotection against chemotherapy-induced reproductive toxicity (Rezvanfar et al. 2013) and UV-induced DNA damage (Prasad et al. 2013), immunomodulatory, anti-inflammatory (Wang et al. 2014), nanomedicinal (Shen et al. 2008), chemotherapeutic and chemoprevention against human melanoma and hepatoma cancers (Chen et al. 2008; Estevez et al. 2014; Peng et al. 2007), biofortification (Durán et al. 2015), and antitumor and anticancer (Jia et al. 2015; Kumar et al. 2015; Mittal et al. 2014; Ren et al. 2013) activities. Other applications include antibacterial, antibiofilm (Bartůněk et al. 2015; Hariharan et al. 2012; Huang et al. 2016; Mittal et al. 2014; Ramya et al. 2015; Shakibaie et al. 2015; Tran and Webster 2011; Wang and Webster 2013), antifungal, antiprotozoan, antitapeworm (Bartůněk et al. 2015), antiviral, wound healing (Ramya et al. 2015), and cytotoxic (Forootanfar et al. 2014; Ramya et al. 2015) activities. Other non-biological activities such as zinc adsorption (Jain et al. 2015), mercury sequestration (Fellowes et al. 2011; Jiang et al. 2012), biosensing of H_2O_2 (Wang et al. 2010), solar cell (Panahi-Kalamuei et al. 2014), and photocatalysis (Triantis et al. 2009; Yang et al. 2008) are also reported.

In this scenario, we have tried to isolate selenite-reducing bacteria in water samples collected from *Pedda cheruvu*, a contaminated lake that receives industrial effluents and domestic sewage. Furthermore, the isolated dominant bacterial strain *AJK3* was identified based on biochemical characterization and 16S rDNA sequencing. The time-dependent selenite removal capability of the isolated strain at different selenite concentrations was monitored with inductively coupled plasma optical emission spectrometry. The selenium nanoparticles produced during bacterial reduction of selenite were studied using different techniques such as UV–visible spectroscopy (UV–Vis), X-ray diffraction (XRD), transmission electron microscopy (TEM), zeta potential measurement, Fourier transform infrared spectroscopy (FTIR), and Raman spectroscopy.

Methods

Materials

Sodium selenite pentahydrate 99% (Sigma-Aldrich, Bengaluru, India), hexamethyldisilazane (Merck, Mumbai, India), nutrient broth and Muller Hinton agar (HiMedia Chemicals Pvt. Ltd., Mumbai, India) were used. At 121 °C for 20 min, all the used glassware, plasticware, and media in the present study were sterilized in Obromax vertical autoclave (Delhi, India). The medium nutrient broth made up of sodium chloride (5 g/L), yeast extract (1.5 g/L), peptone (5 g/L), and beef extract (1.5 g/L). The Mueller–Hinton agar (pH 7.4 ± 0.2) composed of starch (1.5 g/L), beef extract (2 g/L), casein acid hydrolysate (17.5 g/L), and agar (20 g/L). All the solutions were prepared in distilled water. Antibiotic impregnated discs of 6 mm diameter (HiMedia Chemicals Pvt. Ltd,, Mumbai, India) were used for antibiotic susceptibility studies.

Sample collection and bacterial isolation

Surface water samples from *Pedda cheruvu* located at Nacharam, Hyderabad, India (GPS coordinates: 17°25′17.0004″N and 78°33′16.3800″E) were collected in sterile containers. For enumeration and isolation of heterotrophic and selenite-reducing bacteria, the collected water samples were serially diluted in sterile saline and

pour plated on nutrient agar and nutrient agar complemented with 1 mM concentration of sodium selenite, respectively. Petri plates were incubated for 48 h at 37 °C in a Remi CIS-24 Plus orbital shaking incubator (Mumbai, India) and counted for total number of heterotrophic and selenite-reducing bacteria. Among the selenite-reducing bacteria, single colonies were isolated, purified by sub-culturing, and maintained in nutrient broth at 37 °C.

Identification and biochemical characterization

Among the bacterial isolates, the bacterial culture (*AJK3*) that produced intense red colouration on selenite-supplemented nutrient agar was selected for further characterization. This strain was inoculated in nutrient broth and grown overnight under static conditions at 37 °C. The bacterial suspension was prepared from the overnight grown culture by turbidity adjustment to 0.5 McFarland standard, and the prepared suspension was utilized for carrying out the required biochemical and antibiotic susceptibility tests. The following biochemical tests were carried out: motility, catalase, glucose, and mannitol fermentation; nitrate reduction, lecithinase production, indole production, Voges Proskauer's test, and Gram staining in accordance with Bergey's manual of determinative bacteriology (Claus and Berkeley 1986).

The disc diffusion method was used to study the susceptibility of this bacterial strain to various antibiotics. The selected concentrations of antibiotics were gentamicin (10 µg), amikacin (30 µg), streptomycin (10 µg), kanamycin (30 µg), vancomycin (30 µg), erythromycin (15 µg), methicillin (5 µg), chlortetracycline (30 µg), tetracycline (30 µg), ampicillin (10 µg), penicillin G (10 µg), amoxicillin (30 µg), polymyxin B (100 IU), and nalidixic acid (30 µg), respectively. Mueller–Hinton agar plates were inoculated with bacterial suspension and the antibiotic impregnated discs were placed on the medium surface. The sterile empty discs were maintained as negative controls. These petri plates were incubated for 24 h at 37 °C and the inhibition zone was calculated by deducting the diameter of the disc from the diameter of total inhibition zone. The average of three independent experiments was collected.

The size and morphology of the bacterial cells were visualized with scanning electron microscopy technique. The overnight grown bacterial culture was separated from the broth by centrifuging for 10 min at 10,000 rpm. The obtained cell pellet was overnight fixed in glutaraldehyde (2.5%) prepared with phosphate buffer (50 mM, pH 7.2) at 4 °C. The cells were dried serially in graded ethanol solutions of 25, 50, 75 and 100% for 10 min each; suspended in hexamethyldisilazane, and preserved at 4 °C. The obtained suspension was gold sputter coated, after drop coating and air dying on double sided carbon tape. At an accelerating voltage of 20 kV, the samples were observed under Zeiss EVO 18 scanning electron microscope (SEM) (Jena, Germany).

Genomic DNA isolation, amplification, and sequencing of 16S rDNA

Based on the manufacturer's protocol, the genomic DNA from the overnight grown pure culture was isolated with HiPurA bacterial and yeast genomic DNA purification spin kit (HiMedia Chemicals Pvt. Ltd., Mumbai, India). The yield and quality of the isolated DNA was checked on 1% (w/v) agarose gel. The universal primers of *E. coli* 16S rDNA, forward primer (5′-AGAGTTTGATCCTGG CTCAG-3′) and reverse primer (5′-GGTTACCTTGTT ACGACTT-3′), were used to amplify the 16S rRNA gene sequence from the extracted genomic DNA. Eppendorf Mastercycler Pro S (Hamburg, Germany) was employed for carrying out the polymerase chain reaction (PCR), in 25 µL reaction volume containing template DNA (10 ng), Taq DNA polymerase (2.5 units), primers (0.5 µM), 1× buffer containing dNTP (200 µM each) (Bangalore Genei Pvt. Ltd., Bengaluru, India), and $MgCl_2$ (1.5 mM). In each set of experiments, the negative controls were maintained with reaction mix without template DNA. After the initial denaturation (95 °C, 3 min), the 25 PCR cycles were performed for respective time periods at denaturation (95 °C, 1 min), annealing (57 °C, 1 min), extension (72 °C, 2 min), and final extension (72 °C, 5 min) temperatures. The amplified product of ~1500 bp was checked on agarose gel (1.5%) containing ethidium bromide (0.5 µg/mL) with 0.5× TBE buffer, using a low-range 100 bp DNA ruler (Bangalore Genei Pvt. Ltd, Bengaluru, India). As per the manufacturer's guidelines, the amplified products were purified and eluted with HiPurA PCR product purification spin kit (HiMedia Chemicals Pvt. Ltd., Mumbai, India). The sequencing of the purified PCR product was carried out with Applied Biosystems 3730XL genetic Analyzer (Foster City, USA). The obtained 16S rRNA gene sequence of the bacterial strain was compared with the database of GenBank exploiting nucleotide blast search option and the matched sequences were downloaded. Based on the scoring index, using CLUSTAL W, a multiple sequence alignment program, the most similar sequences were organized. The software version Molecular Evolutionary Genetics Analysis (MEGA) 5.1 was utilized for constructing the phylogenetic tree by the neighbor-joining method for showing the relationship between isolated strain (*AJK3*) and the other bacterial species (Joshi et al. 2011). The 16S rDNA sequence of *AJK3* was deposited in GenBank.

Reduction of selenite and synthesis of selenium nanoparticles

The medium nutrient broth complemented with various sodium selenite concentrations was inoculated with bacterial suspension (100 µL of 10^7 CFU/mL) and grown under static conditions at 37 °C in Remi CIS-24 Plus bacteriological incubator (Mumbai, India). The synthesis was inspected by recording the culture broth's UV–Vis absorption spectra and for visual colour change at specified time periods. The role of metalloid concentration (0.25–1.0 mM) and incubation duration (24–72 h) on reductive nanoparticle production was monitored. The culture medium was separated from the bacterial cells and the nanoparticles by centrifugation at 16,750×*g* for 10 min. With Horiba Jobin–Yvon JY-2000 inductively coupled plasma optical emission spectrometry (ICP-OES) (Longjumeau, France), the selenium metal concentration in the culture supernatants was quantified.

Selenium nanoparticle characterization

The UV–visible absorption spectra of the selenium nanoparticle containing culture broth were recorded periodically at regular intervals (24, 48 and 72 h) using a Analytic Jena AG Specord 200 Plus UV–visible spectrophotometer (Jena, Germany), at a wavelength range of 350–900 nm. The 72 h-grown bacterial cells in 1 mM selenite enriched nutrient broth which contain the nanoparticles were separated from the culture medium by centrifugation (16,750×*g*, 10 min) in Remi R-24 laboratory centrifuge (Mumbai, India). The washed cell pellets were suspended in chilled sodium phosphate buffer (100 mM, pH 7.4). The cell suspension was disrupted by ice sonication with Sonics Vibra Cell VC 750 ultrasonicator (Newtown, USA) for 4 min (4 s pulse, 2 s pause), at an amplitude of 40%. The obtained slurry was washed and stored in sterile water. At 40 kV and 30 mA, the X-ray diffraction study was carried out with a Rigaku, Ultima IV diffractometer (Tokyo, Japan) using monochromatic Cu Kα radiation ($\lambda = 1.5406$ Å). At a scan rate of 1°/min, the intensity data were collected in the range of 20–100° 2θ, for the nanocolloid solution drop coated on a glass slide. At 633 nm excitation wavelength, the Raman spectrum of the nanoparticles under room temperature was collected with a Horiba Jobin–Yvon LabRAM HR 800 micro-Raman spectrometer (Longjumeau, France). At 200 kV, the morphology of the nanoparticles drop coated on carbon-coated copper grids was obtained with FEI Tecnai 20 G2 S-Twin (Eindhoven, The Netherlands) transmission electron microscope (TEM) coupled to INCAx-act Oxford Instruments Energy-Dispersive X-ray (EDX) (High Wycombe, UK). The zeta potential of the nanoparticles suspended in ultra pure water was evaluated by a Malvern Zetasizer Nano ZS90 (Malvern, UK). Using an FTS Systems Dura-Dry™ MP freeze dryer (New York, USA), the nanoparticle solutions were made into powders. Using Bruker Optics TENSOR 27 FTIR spectrometer (Ettlingen, Germany), the IR spectra of the lyophilized powders were noted at a wave number range of 1000–4000 cm^{-1}.

The selenite reduction activity of the strain was studied for different cellular fractions (cytosolic and membrane), along with the culture supernatant. The cell pellet and supernatant were obtained by centrifuging the nutrient broth grown overnight culture. The washed cell pellet suspended in chilled phosphate buffer was disrupted by ice sonication. The obtained cell lysate was centrifuged to separate the soluble and membrane fractions. The total protein content was quantified by Bradford method using BSA as standard. The selenite reductase activity was carried out at 37 °C for 24 h in 400 µL of supernatant or nutrient broth containing 100 µg of protein and 1 mM sodium selenite. The reaction mixtures without supernatant or protein fractions served as controls (Dhanjal and Cameotra 2010; Lampis et al. 2014).

Results and discussion

Characterization and identification of selenite-reducing bacterial strain

It is well documented that the contaminated sites are the potent sources for competent bacteria that are naturally adapted to the local environment (Ghosh et al. 2008). Thus, an effort has been made to isolate selenite-reducing bacteria from *Pedda Cheruvu*, a contaminated lake located at Nacharam, Hyderabad, India. The lake receives effluents from the manufacturing industries such as steel, chemicals, paints, rubber, plastics, breweries, and food products located at industrial development area (IDA) of Nacharam; agricultural wastes and domestic sewage. In addition, contamination of the ground and surface waters, soil, and sediments of the lake with heavy metals has been reported (Govil et al. 1999; Udayalaxmi et al. 2010; Venkateswara Rao et al. 2016). The collected water samples were analyzed for heterotrophic and selenite-reducing bacteria, and the respective counts were 9.1×10^6 and 8.2×10^5 CFU/mL. Among the purified bacterial isolates from surface waters of the lake, a dominant bacterial strain (*AJK3*) that produced intense red colouration on selenite-supplemented nutrient agar was selected for further characterization. For identifying the phenotypical characteristics of this strain, various biochemical tests were performed. The strain *AJK3* was Gram-positive, motile, and produced large, white coloured granular colonies of 2–5 mm diameter on nutrient agar. The colonies were dark red in colour on selenite-supplemented nutrient agar medium. In addition, the selenite-supplemented broth's colour changed from dull

yellow to red (Fig. 1a–c). Similarly, the size and morphological features of the isolated bacterial strain *AJK3* were visualized with SEM technique (Fig. 1d). From the micrograph, it is evident that the bacterial strain is rod shaped and the size is 1.3 (L) × 0.6 (W) µm. The strain showed positive result for key characteristics such as catalase production, glucose fermentation, nitrate reduction, lecithinase production, polymyxin resistance, Voges Proskauer's test, and inability to ferment mannitol and produce indole. Depended on the morphological, biochemical, and physiological characteristics, the strain *AJK3* was tentatively recognized as *Bacillus* sp. Further confirmation was obtained from the comparative analysis of the 16S rDNA sequence. Under the accession No MF187726, a 1010 nucleotide long 16S rDNA sequence from *AJK3* was deposited in NCBI database. The 16S rRNA gene sequence analysis revealed highest sequence similarity (98%) with *B. cereus* strains. Based on the results, the bacterial strain *AJK3* has been classified as *B. cereus* and the phylogenetic tree is depicted in Fig. 2. The occurrence of *B. cereus* in surface waters, faecal polluted rivers, sewage, and diary industry waste is reported in the literature (Østensvik et al. 2004).

The sensitivity of the isolate towards various aminoglycosidic (amikacin, gentamicin, kanamycin, and streptomycin), beta-lactam (amoxicillin, methicillin, ampicillin, and penicillin G), macrolide (erythromycin), polyketide (tetracycline and chlortetracycline), cationic peptide (polymyxin B), glycopeptides (vancomycin), and quinolone (nalidixic acid) antibiotics was tested (Fig. 3).

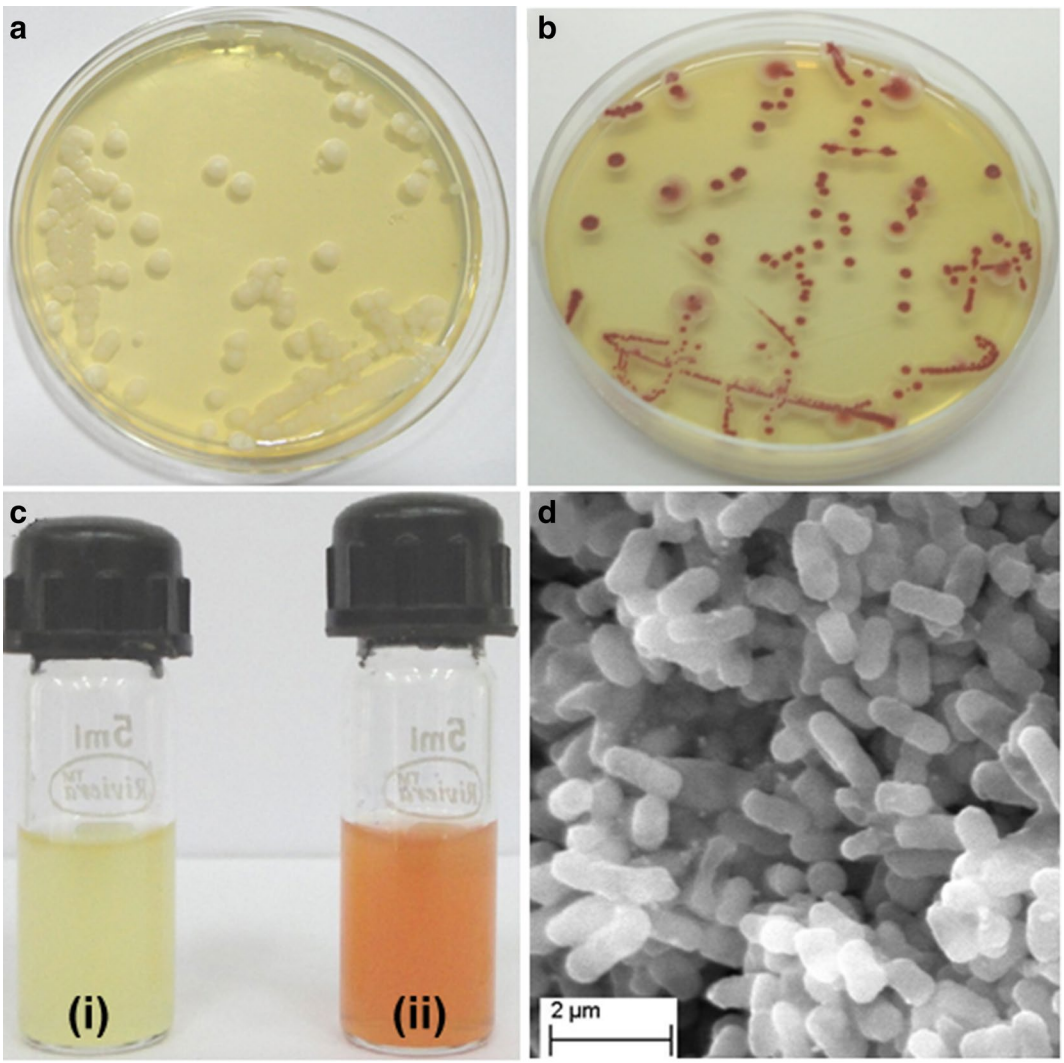

Fig. 1 Bacterial culture plates showing single colonies of *AJK3* strain on **a** nutrient agar and **b** nutrient agar supplemented with 1 mM selenite. **c** Colour of the bacterial culture broth (i) without and (ii) with selenite supplementation and **d** SEM image of bacterial cells

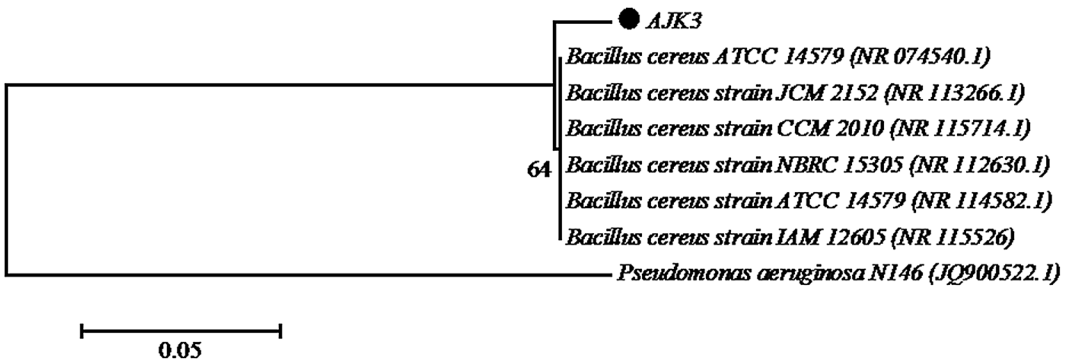

Fig. 2 Dendrogram showing the phylogenetic relationship between the partial 16S rRNA gene sequences of the isolate *AJK3* and related bacterial species. The scale bar indicates the sequence divergence. The strain *Pseudomonas aeruginosa* N146 was used as an outgroup

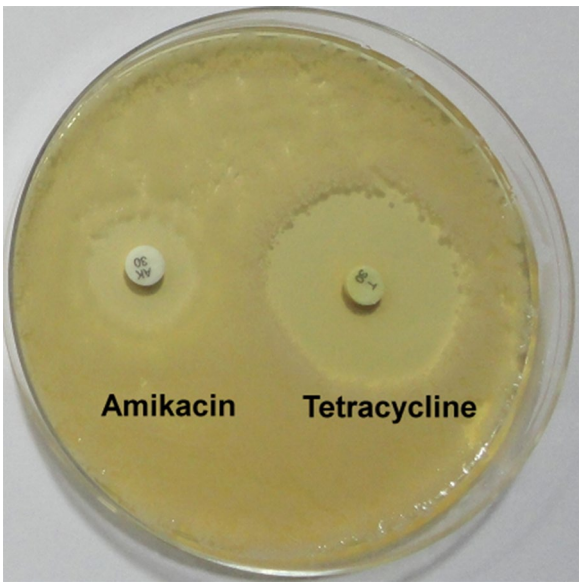

Fig. 3 Bacterial culture plate of *AJK3* strain showing the inhibition zones around the discs loaded with 30 µg of antibiotics

Table 1 Antibiotic sensitivity of *AJK3* strain

Antibiotic (µg/disc)	ZOI (mm)
Amikacin (30)	10.5 ± 0.5
Gentamicin (10)	8.6 ± 0.5
Kanamycin (30)	9.2 ± 0.4
Streptomycin (10)	12.4 ± 0.5
Vancomycin (30)	13.6 ± 0.5
Polymyxin B (100)	0 ± 0
Erythromycin (15)	9.0 ± 0.0
Tetracycline (30)	26.6 ± 1.5
Chlortetracycline (30)	26.0 ± 1.6
Methicillin (5)	8.2 ± 1.3
Ampicillin (10)	19.8 ± 2.0
Penicillin G (10)	18.6 ± 0.8
Amoxicillin (30)	14.4 ± 0.5
Nalidixic acid (30)	20.7 ± 0.9

Table 2 Time-dependent selenium removal (%) by *AJK3* at different selenite concentrations

Selenite concentration (mM)	Selenium removal (%)		
	Time (h)		
	24	48	72
0.25	31.72 ± 0.25	50.97 ± 1.20	43.86 ± 1.12
0.5	35.15 ± 2.49	78.50 ± 2.50	67.56 ± 2.15
1.0	3.69 ± 1.87	82.73 ± 2.87	84.23 ± 1.86

The strain showed resistance to gentamicin, kanamycin, methicillin, erythromycin, polymyxin B, and intermediate sensitivity to amikacin, streptomycin, amoxicillin, vancomycin, and high sensitivity to ampicillin, penicillin, tetracycline, chlortetracycline, and nalidixic acid antibiotics (Table 1).

Selenite reduction and biogenesis of selenium nanoparticles

The selenite reduction capability of the strain *AJK3* was determined by quantifying the selenium content in the culture supernatants at different concentrations (Table 2). At a lower concentration of 0.25 mM selenite, 51% of selenium removal was noted within 48 h with further no increase from 48 to 72 h. At 48 h, the selenium removal (%) was increased from 35.15 to 78.5 and reached saturation (67.56) at 72 h at 0.5 mM selenite. The selenium removal (%) was only 3.69 at 24 h, increased to 82.73 at 48 h, and remained more or less same (84.23) at 72 h, at a higher concentration of 1 mM selenite. This could be due to a lag in detoxifying enzyme induction which is

required for selenite tolerance at higher concentrations. The selenium nanoparticle formation in the culture broth was observed visually and by UV–Vis. With increase in time, the colour of the selenite-supplemented culture broth changed from pale yellow to red, a signature for the reduction of selenite to elemental selenium (Fig. 1c). The characteristic red colour could be accounted for the surface plasmon resonance of selenium nanoparticles. The time-dependent nanoparticle synthesis was measured with UV–Vis at various selenium oxyanion concentrations (0.25, 0.5, and 1.0 mM) (Fig. 4). The culture broths showed broad absorption bands at all the tested concentrations in the range of 350–900 nm. At a concentration of 0.25 mM selenite, the absorption band increased from 48 to 72 h. In the case of higher concentrations (0.5 and 1 mM selenite), the intensities of the absorption bands increased from 24 to 48 h and remained more or less same at 72 h. In addition, the observed time-dependent increase in absorption was in concomitance with enhanced red hue of the culture broth. However, no colour change was observed in control experiment carried out with selenite-supplemented nutrient broth without bacterial inoculation. Thus, the selenium nanoparticle synthesis is attributed to bacterial reduction of selenite only. It is reported in the literature that the biogenic selenium nanoparticles exhibit different spectroscopic characteristics in comparison with chemogenic selenium nanoparticles due to unique internal structural arrangements of the selenium atoms (Oremland et al. 2004). Thus, the bacterial strain used in the current study can be utilized as a nanofactory for large-scale commercial production of selenium nanoparticles.

It is significant to note that, in the literature, selenium nanoparticle producing bacteria are reported in wide range of environments under aerobic and anaerobic conditions including in sludge and sewerage (Mishra et al. 2011). The anaerobic/anoxic bacteria include strains such as *Selenihalanaerobacter shriftii* DSSE1, *Sulfurospirillum barnesii* (Oremland et al. 2004), *Rhodopseudomonas palustris* N (Li et al. 2014), *Veillonella atypica* (Pearce et al. 2008), *Shewanella putrefaciens* 200 (Jiang et al. 2012), *Shewanella* sp. HN-41 (Lee et al. 2007), etc. In

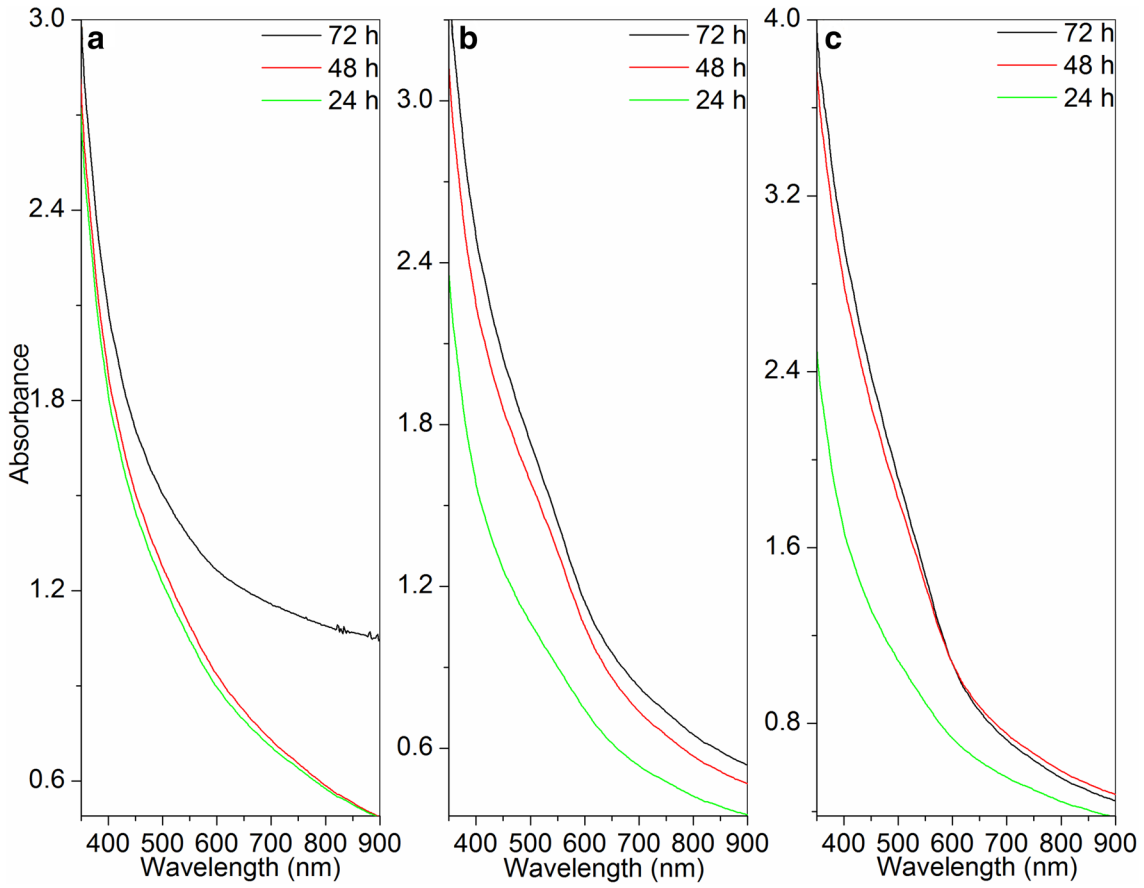

Fig. 4 Time-dependent UV–Vis absorption spectra of selenium nanoparticles synthesized by strain *AJK3* at various selenite concentrations: **a** 0.25 mM, **b** 0.5 mM, and **c** 1.0 mM

comparison with the anaerobic bacteria, the phenomenon is mostly cited in aerobic, Gram +ve *Bacillus* species such as *B. cereus* (Dhanjal and Cameotra 2010), *Bacillus* sp. MSh-1 (Shakibaie et al. 2015), *B. megaterium* (Mishra et al. 2011), *B. mycoides* SeITE01 (Lampis et al. 2014), *Bacillus* sp. E5 (Durán et al. 2015), *B. licheniformis* (Khiralla and El-Deeb 2015), *B. subtilis* (Wang et al. 2010), etc. Other reported aerobic strains are *Pseudomonas agglomerans*, (Torres et al. 2012), *P. aeruginosa* JS-11 (Dwivedi et al. 2013), *P. stutzeri* (Lortie et al. 1992), *P. alcaliphila* (Zhang et al. 2011), *Duganella* sp., *Agrobacterium* sp. (Bajaj et al. 2012), *Zooglea ramigera* (Srivastava and Mukhopadhyay 2013), *Streptomyces minutiscleroticus* M10A62 (Ramya et al. 2015), *Acinetobacter* sp. E6.2 (Durán et al. 2015), *Comamonas testosteroni* S44 (Zheng et al. 2014), *Klebsiella pneumonia* (Fesharaki et al. 2010), *Lactobacillus* sp, *Bifidobacter* sp., and *Streptococcus thermophilus* (Eszenyi et al. 2011).

Crystallographic structure of selenium nanoparticles

The crystallographic structure of the generated nanoparticles was established from the XRD. The XRD pattern was broader with no sharp Bragg reflections (Fig. 5a). Hence, the red-coloured selenium nanoparticles produced by bacterial reduction are amorphous in structure. Furthermore, the recorded Raman spectrum of the nanoparticles is given in Fig. 5b. The spectrum showed two characteristic resonance peaks at 234 and 254 cm^{-1}, which could be attributed to amorphous (Van Overschelde et al. 2013) and trigonal selenium (Liu et al. 2008), respectively. The trigonal selenium could have formed via phase transformation of amorphous selenium to trigonal selenium by powerful Raman laser beam during measurement (Liu et al. 2008). Besides, the broadened Raman bands also explain the nanosize effect of the produced nanoparticles (Shikuo et al. 2007). Thus, the Raman data validate the amorphous crystal structure of the nanoparticles obtained from the XRD pattern. The present study on amorphous state of synthesized nanoparticles is in agreement with the previous studies carried out on bacterial biosynthesis of selenium nanoparticles with *Shewanella* sp. HN-41 (Tam et al. 2010), *Bacillus* sp. (Shakibaie et al. 2010), *Escherichia coli* K-12 (Dobias et al. 2011), *P. alcaliphila* (Zhang et al. 2011), and *Pantoea agglomerans* (Torres et al. 2012). It is well known that the selenium nanoparticles generated by biological reduction are, indeed, characteristically amorphous in nature (Torres et al. 2012).

Morphology and size of selenium nanoparticles

The TEM images of nanoparticles synthesized with 1 mM selenite-supplemented nutrient broth at 72 h of time is given in Fig. 6. The produced nanoparticles were sphere shaped and polydisperse. The size of the particles varied from 50 to 150 nm and the mean particle size was about 92.6 ± 20.6 nm, obtained from the respective diameter distribution (Fig. 6b). These results are compared with earlier study carried out on biosynthesis of selenium nanoparticles with marine bacterial strain *Bacillus* sp. MSh-1, in which nanoparticles in size range of about 80–220 nm were obtained (Forootanfar et al. 2014), while the probiotic lactic acid bacteria such as *Lactobacillus* and *Bifidobacter* produced selenium nanoparticles in the size ranges of 100–200 and 400–500 nm, respectively (Eszenyi et al. 2011). From the data, it is evident that the strain *B. cereus* is able to produce selenium nanoparticles with smaller average nanoparticle size and narrow particle size distribution. The shown selected area

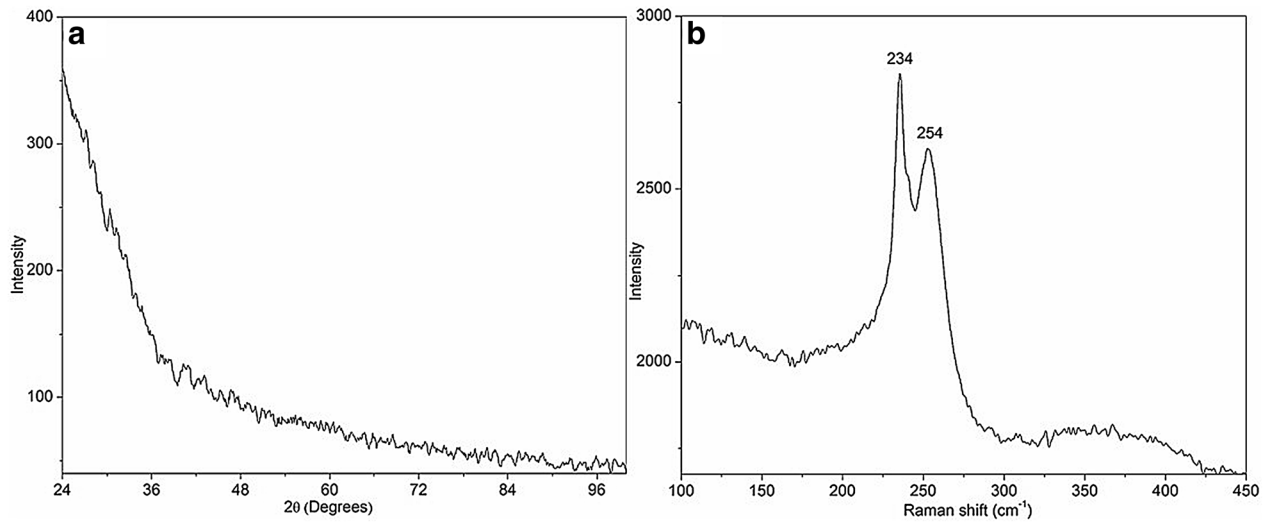

Fig. 5 **a** X-ray diffraction pattern and **b** Raman spectrum of selenium nanoparticles

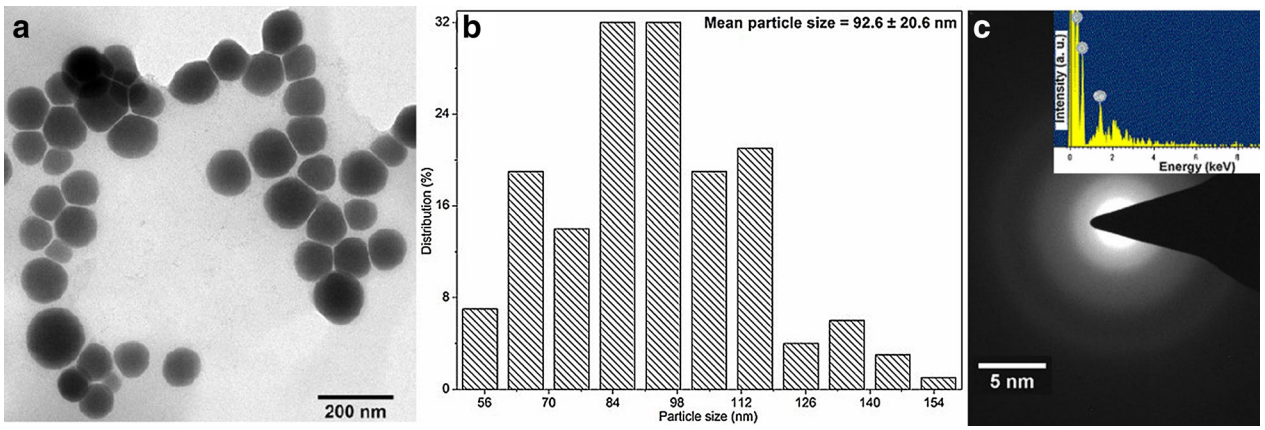

Fig. 6 **a** TEM image of selenium nanoparticles synthesized with 1 mM selenite at 72 h, **b** histogram showing the particle size distribution, and **c** corresponding SAED pattern

electron diffraction (SAED) pattern is diffused (Fig. 6c) and also confirms the amorphous character of the bacteriogenic nanoparticles supported from the Raman spectroscopy and XRD. In addition, the EDX spectrum corroborates the selenium presence in the nanoparticles (inset of Fig. 6c). The nanoparticles exhibit absorption peak at 1.37 keV, attribute to the characteristic absorption of SeLα. The extra peaks of carbon and oxygen can be pointed to the protein molecules. The zeta potential of the synthesized selenium nanoparticles suspended in ultrapure water was found to be -31.1 ± 4.9 mV. The higher negative charge on the nanoparticle surface is due to capping and stabilization of nanoparticles by bacterial proteins (Dhanjal and Cameotra 2010).

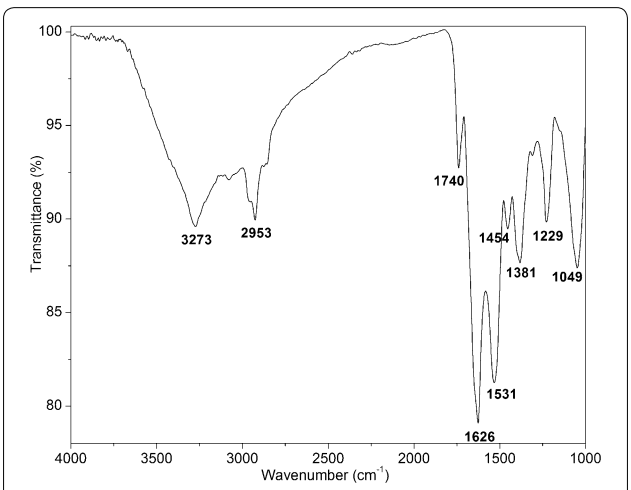

Fig. 7 FTIR spectrum of freeze-dried selenium nanoparticles

Involvement of biomolecules in synthesis and stabilization of nanoparticles

The functional groups of the bacterial biomolecules acting as reducing and capping agents during the nanoparticle production were identified from the IR spectrum (Fig. 7). The major absorbance bands in the nanoparticle spectrum were at 3273, 2953, 1740, 1626, 1531, 1454, 1381, 1229, and 1049 cm^{-1}. The stretching vibrations of O–H groups could be assigned to broad band noted at 3273 cm^{-1}. The band at 2953 cm^{-1} corresponds to asymmetric stretches of methylene groups. The carbonyl-stretching vibrations in aldehydes, ketones, and carboxylic acids could be assigned to sharp band found at 1740 cm^{-1}. The amide I and amide II linkages can be recognized at observed bands at 1626 and 1531 cm^{-1}. They correspond to the vibrations of carbonyl and N–H stretches in the amide linkages of the proteins, respectively. The symmetrical stretch of carboxylate group can be attributed to the bands observed at 1454 and 1381 cm^{-1}. The C–O stretch of carboxylic acids corresponds to peak at 1229 cm^{-1}. The C–O stretches of ether groups were noted at 1049 cm^{-1}. The involvement of proteins in the reduction and stabilization of selenium nanoparticles was reported in biosynthesis of selenium nanoparticles using bacteria *Streptomyces minutiscleroticus* M10A62 (Ramya et al. 2015) and *P. alcaliphila* (Zhang et al. 2011).

The localization of selenite reductase activity was determined using selenite-amended culture supernatant, soluble, and membrane protein fractions (Fig. 8a). In the current study, the selenite reduction was noted only in the membrane protein fraction and supernatant. Thus, the results confirm that the extracellular proteins released by the bacterial cells and the proteins associated with membrane/cell wall are involved in the metalloid reduction (Lampis et al. 2014). These proteins probably act as oxidation–reduction enzymes or proton antitransporters (Zhang et al. 2011). It is also evident from

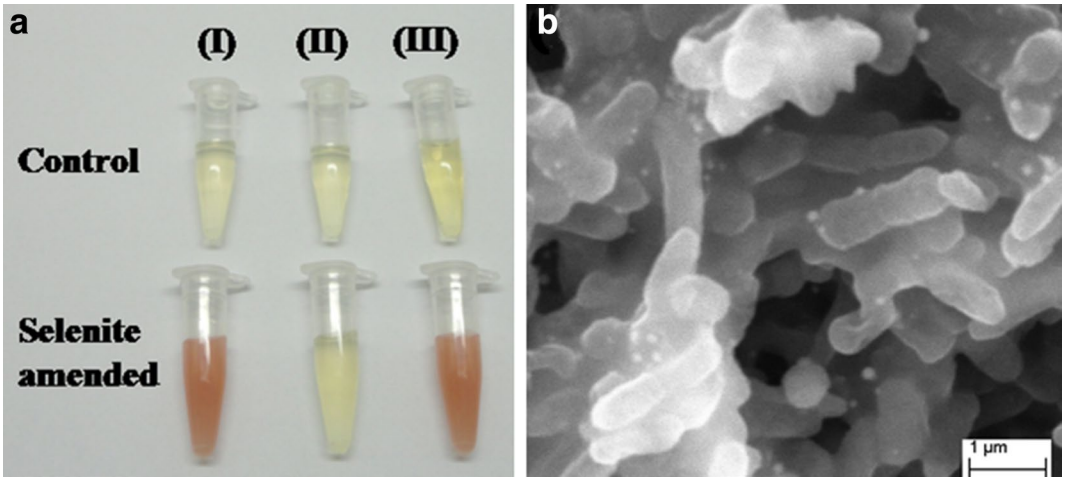

Fig. 8 **a** Localization of selenite reductase activity in various fractions of control and selenite-amended reaction mixtures; (I) Supernatant, (II) cytosolic, and (III) membrane fractions and **b** SEM picture indicating the selenium nanospheres adhered bacterial cells

the scanning electron micrograph, in which the bacterial cells are adhered by the selenium nanospheres (Fig. 8b).

Conclusions

In the current investigation, selenite-reducing bacterial strain *AJK3* was isolated from the native bacterial population of a polluted lake. Based on biochemical characterization and 16S rDNA sequencing, the strain was identified as *B. cereus*. The method of bacteriogenic synthesis of selenium nanoparticle was studied at different selenite concentrations with time. The strain was able to produce amorphous, spherical nanoparticles of 93 nm. Thus, the isolated bacterial strain can be exploited as a prospective, renewable, natural, nanofactory for the bacteriogenic synthesis of nanoparticles, in addition to the detoxification of selenite from the contaminated environment. Further detailed studies are envisaged on enzymatic detoxification mechanisms of metalloid reduction, other products of selenite biotransformation such as seleno-amino acids and volatile alkyl selenides; scale up for commercial production; biological activities of the produced selenium nanoparticles (Eswayah et al. 2016; Nancharaiah and Lens 2015).

Authors' contributions

The author alone involved in carrying out all the experiments, writing, and interpretation of results during preparation of the manuscript. The author read and approved the final manuscript.

Acknowledgements

The author would like to thank Dr. A. C. Sahayam, Head, Bulk Analysis Section, and Dr. Sunil Jai Kumar, Head of the Division, NCCCM, BARC for their continuing encouragement and support during the study.

Competing interests

The author declares that she has no competing interests.

Availability of data and materials

The data set supporting the conclusions of this article is included within the article. The author has agreed to provide the data and materials.

Consent for publication

Not applicable.

Ethics approval and consent to participate

Not applicable.

Funding

No funding source to declare.

Publisher's Note

Received: 19 March 2018 Accepted: 18 June 2018
Published online: 25 June 2018

References

Bajaj M, Schmidt S, Winter J (2012) Formation of Se (0) nanoparticles by *Duganella* sp. and *Agrobacterium* sp. isolated from Se-laden soil of North-East Punjab, India. Microb Cell Factories 11:14

Bartůněk V, Junková J, Šuman J, Kolářová K, Rimpelová S, Ulbrich P, Sofer Z (2015) Preparation of amorphous antimicrobial selenium nanoparticles stabilized by odor suppressing surfactant polysorbate 20. Mater Lett 152:207–209. https://doi.org/10.1016/j.matlet.2015.03.092

Chen T, Wong Y-S, Zheng W, Bai Y, Huang L (2008) Selenium nanoparticles fabricated in *Undaria pinnatifida* polysaccharide solutions induce mitochondria-mediated apoptosis in A375 human melanoma cells. Colloid Surf B 67:26–31. https://doi.org/10.1016/j.colsurfb.2008.07.010

Claus D, Berkeley RCW (1986) Genus *Pseudomonas*. In: Sneath PHA, Mair NS, Sharpe ME (eds) Bergey's manual of determinative bacteriology, vol 1. Williams & Wilkins, Baltimore, pp 140–219

Dhanjal S, Cameotra SS (2010) Aerobic biogenesis of selenium nanospheres by *Bacillus cereus* isolated from coalmine soil. Microb Cell Factories 9:11

Dobias J, Suvorova EI, Bernier-Latmani R (2011) Role of proteins in controlling selenium nanoparticle size. Nanotechnol 22:195605
Durán P, Acuña JJ, Gianfreda L, Azcón R, Funes-Collado V, Mora ML (2015) Endophytic selenobacteria as new inocula for selenium biofortification. Appl Soil Ecol 96:319–326. https://doi.org/10.1016/j.apsoil.2015.08.016
Dwivedi S, AlKhedhairy AA, Ahamed M, Musarrat J (2013) Biomimetic synthesis of selenium nanospheres by bacterial strain JS-11 and its role as a biosensor for nanotoxicity assessment: a novel Se-bioassay. PLoS ONE 8:e57404
Estevez H, Garcia-Lidon JC, Luque-Garcia JL, Camara C (2014) Effects of chitosan-stabilized selenium nanoparticles on cell proliferation, apoptosis and cell cycle pattern in HepG2 cells: comparison with other *seleno* species. Colloid Surf B 122:184–193. https://doi.org/10.1016/j.colsurfb.2014.06.062
Eswayah AS, Smith TJ, Gardiner PH (2016) Microbial transformations of selenium species of relevance to bioremediation. Appl Environ Microbiol 82:4848–4859. https://doi.org/10.1128/aem.00877-16
Eszenyi P, Sztrik A, Babka B, Prokisch J (2011) Elemental, nano-sized (100–500 nm) selenium production by probiotic lactic acid bacteria. Int J Biosc Biochem Bioinfo 1:148–152
Fellowes JW, Pattrick RAD, Green DI, Dent A, Lloyd JR, Pearce CI (2011) Use of biogenic and abiotic elemental selenium nanospheres to sequester elemental mercury released from mercury contaminated museum specimens. J Hazard Mater 189:660–669. https://doi.org/10.1016/j.jhazmat.2011.01.079
Fesharaki PJ, Nazari P, Shakibaie M, Rezaie S, Banoee M, Abdollahi M, Shahverdi AR (2010) Biosynthesis of selenium nanoparticles using *Klebsiella pneumoniae* and their recovery by a simple sterilization process. Braz J Microbiol 41:461–466
Forootanfar H, Adeli-Sardou M, Nikkhoo M, Mehrabani M, Amir-Heidari B, Shahverdi AR, Shakibaie M (2014) Antioxidant and cytotoxic effect of biologically synthesized selenium nanoparticles in comparison to selenium dioxide. J Trace Elem Med Biol 28:75–79. https://doi.org/10.1016/j.jtemb.2013.07.005
Ghosh A, Mohod AM, Paknikar KM, Jain RK (2008) Isolation and characterization of selenite- and selenate-tolerant microorganisms from selenium-contaminated sites. World J Microbiol Biotechnol 24:1607–1611. https://doi.org/10.1007/s11274-007-9624-z
Govil PK, Reddy GLN, Gnaneswara Rao T (1999) Environmental pollution in India-Heavy metals and radiogenic elements in Nacharam lake. Environ Health 61:23
Hariharan H, Al-Harbi NA, Karuppiah P, Rajaramam SK (2012) Microbial synthesis of selenium nanocomposite using *Saccharomyces cerevisiae* and its antimicrobial activity against pathogens causing nosocomial infection. Chalcogenide Lett 9:509–515
Huang B, Zhang J, Hou J, Chen C (2003) Free radical scavenging efficiency of Nano-Se in vitro Free Rad Biol Med 35:805–813. https://doi.org/10.1016/S0891-5849(03)00428-3
Huang X, Chen X, Chen Q, Yu Q, Sun D, Liu J (2016) Investigation of functional selenium nanoparticles as potent antimicrobial agents against superbugs. Acta Biomater 30:397–407. https://doi.org/10.1016/j.actbio.2015.10.041
Husen A, Siddiqi KS (2014) Plants and microbes assisted selenium nanoparticles: characterization and application. J Nanobiotechnol 12:28
Jain R et al (2015) Adsorption of zinc by biogenic elemental selenium nanoparticles. Chem Eng J 260:855–863. https://doi.org/10.1016/j.cej.2014.09.057
Jia X, Liu Q, Zou S, Xu X, Zhang L (2015) Construction of selenium nanoparticles/β-glucan composites for enhancement of the antitumor activity. Carbohydr Polym 117:434–442. https://doi.org/10.1016/j.carbpol.2014.09.088
Jiang S, Ho CT, Lee J-H, Duong HV, Han S, Hur H-G (2012) Mercury capture into biogenic amorphous selenium nanospheres produced by mercury resistant *Shewanella putrefaciens* 200. Chemosphere 87:621–624. https://doi.org/10.1016/j.chemosphere.2011.12.083
Joshi MH, Balamurugan P, Venugopalan VP, Rao TS (2011) Dense fouling in acid transfer pipelines by an acidophilic rubber degrading fungus. Biofouling 27:621–629. https://doi.org/10.1080/08927014.2011.594162
Khiralla GM, El-Deeb BA (2015) Antimicrobial and antibiofilm effects of selenium nanoparticles on some foodborne pathogens. LWT Food Sci Technol 63:1001–1007. https://doi.org/10.1016/j.lwt.2015.03.086
Kong H, Yang J, Zhang Y, Fang Y, Nishinari K, Phillips GO (2014) Synthesis and antioxidant properties of gum arabic-stabilized selenium nanoparticles. Int J Biol Macromol 65:155–162. https://doi.org/10.1016/j.ijbiomac.2014.01.011
Kumar S, Tomar MS, Acharya A (2015) Carboxylic group-induced synthesis and characterization of selenium nanoparticles and its anti-tumor potential on Dalton's lymphoma cells. Colloid Surf B 126:546–552. https://doi.org/10.1016/j.colsurfb.2015.01.009
Lampis S, Zonaro E, Bertolini C, Bernardi P, Butler CS, Vallini G (2014) Delayed formation of zero-valent selenium nanoparticles by *Bacillus mycoides* SeITE01 as a consequence of selenite reduction under aerobic conditions. Microb Cell Factories 13:35
Lee J-H, Han J, Choi H, Hur H-G (2007) Effects of temperature and dissolved oxygen on Se(IV) removal and Se(0) precipitation by *Shewanella sp*. HN-41. Chemosphere 68:1898–1905. https://doi.org/10.1016/j.chemosphere.2007.02.062
Li B et al (2014) Reduction of selenite to red elemental selenium by *Rhodopseudomonas palustris* strain N. PLoS ONE 9:e95955
Liu L, Peng Q, Li Y (2008) Preparation of monodisperse Se colloid spheres and Se nanowires using Na_2SeSO_3 as precursor. Nano Res 1:403–411. https://doi.org/10.1007/s12274-008-8040-5
Lortie L, Gould WD, Rajan S, McCready RGL, Cheng KJ (1992) Reduction of selenate and selenite to elemental selenium by a *Pseudomonas stutzeri* isolate. Appl Environ Microbiol 58:4042–4044
Mishra RR, Prajapati S, Das J, Dangar TK, Das N, Thatoi H (2011) Reduction of selenite to red elemental selenium by moderately halotolerant *Bacillus megaterium* strains isolated from Bhitarkanika mangrove soil and characterization of reduced product. Chemosphere 84:1231–1237. https://doi.org/10.1016/j.chemosphere.2011.05.025
Mittal AK, Kumar S, Banerjee UC (2014) Quercetin and gallic acid mediated synthesis of bimetallic (silver and selenium) nanoparticles and their antitumor and antimicrobial potential. J Colloid Interf Sci 431:194–199. https://doi.org/10.1016/j.jcis.2014.06.030
Nancharaiah YV, Lens PNL (2015) Ecology and biotechnology of selenium-respiring bacteria. Microbiol Mol Biol Rev MMBR 79:61–80. https://doi.org/10.1128/MMBR.00037-14
Oremland RS et al (2004) Structural and spectral features of selenium nanospheres produced by Se-respiring bacteria. Appl Environ Microbiol 70:52–60. https://doi.org/10.1109/bmn.2003.1220609
Østensvik Ø, From C, Heidenreich B, O'Sullivan K, Granum PE (2004) Cytotoxic *Bacillus* spp. belonging to the *B. cereus* and *B. subtilis* groups in Norwegian surface waters. J Appl Microbiol 96:987–993. https://doi.org/10.1111/j.1365-2672.2004.02226.x
Panahi-Kalamuei M, Salavati-Niasari M, Hosseinpour-Mashkani SM (2014) Facile microwave synthesis, characterization, and solar cell application of selenium nanoparticles. J Alloys Compd 617:627–632. https://doi.org/10.1016/j.jallcom.2014.07.174
Pearce CI et al (2008) Microbial manufacture of chalcogenide-based nanoparticles via the reduction of selenite using *Veillonella atypica*: an in situ EXAFS study. Nanotechnol 19:155603
Peng D, Zhang J, Liu Q, Taylor EW (2007) Size effect of elemental selenium nanoparticles (Nano-Se) at supranutritional levels on selenium accumulation and glutathione S-transferase activity. J Inorg Biochem 101:1457–1463. https://doi.org/10.1016/j.jinorgbio.2007.06.021
Prasad KS, Patel H, Patel T, Patel K, Selvaraj K (2013) Biosynthesis of Se nanoparticles and its effect on UV-induced DNA damage. Colloid Surf B 103:261–266. https://doi.org/10.1016/j.colsurfb.2012.10.029
Ramya S, Shanmugasundaram T, Balagurunathan R (2015) Biomedical potential of actinobacterially synthesized selenium nanoparticles with special reference to anti-biofilm, anti-oxidant, wound healing, cytotoxic and anti-viral activities. J Trace Elem Med Biol 32:30–39. https://doi.org/10.1016/j.jtemb.2015.05.005
Ren Y et al (2013) Antitumor activity of hyaluronic acid–selenium nanoparticles in Heps tumor mice models. Int J Biol Macromol 57:57–62. https://doi.org/10.1016/j.ijbiomac.2013.03.014
Rezvanfar MA, Rezvanfar MA, Shahverdi AR, Ahmadi A, Baeeri M, Mohammadirad A, Abdollahi M (2013) Protection of cisplatin-induced spermatotoxicity, DNA damage and chromatin abnormality by selenium nano-particles. Toxicol Appl Pharmacol 266:356–365. https://doi.org/10.1016/j.taap.2012.11.025
Shakibaie M, Khorramizadeh MR, Faramarzi MA, Sabzevari O, Shahverdi AR (2010) Biosynthesis and recovery of selenium nanoparticles and the effects on

matrix metalloproteinase-2 expression. Biotechnol Appl Biochem 56:7–15. https://doi.org/10.1042/ba20100042
Shakibaie M, Forootanfar H, Golkari Y, Mohammadi-Khorsand T, Shakibaie MR (2015) Anti-biofilm activity of biogenic selenium nanoparticles and selenium dioxide against clinical isolates of *Staphylococcus aureus*, *Pseudomonas aeruginosa*, and *Proteus mirabilis*. J Trace Elem Med Biol 29:235–241. https://doi.org/10.1016/j.jtemb.2014.07.020
Shen Y, Wang X, Xie A, Huang L, Zhu J, Chen L (2008) Synthesis of dextran/Se nanocomposites for nanomedicine application. Mater Chem Phys 109:534–540. https://doi.org/10.1016/j.matchemphys.2008.01.016
Shikuo L, Yuhua S, Anjian X, Xuerong Y, Xiuzhen Z, Liangbao Y, Chuanhao L (2007) Rapid, room-temperature synthesis of amorphous selenium/protein composites using *Capsicum annuum* L. extract. Nanotechnol 18:405101
Srivastava N, Mukhopadhyay M (2013) Biosynthesis and structural characterization of selenium nanoparticles mediated by *Zooglea ramigera*. Powder Technol 244:26–29. https://doi.org/10.1016/j.powtec.2013.03.050
Tam K et al (2010) Growth mechanism of amorphous selenium nanoparticles synthesized by *Shewanella* sp. HN-4. Biosci Biotechnol Biochem 74:696–700
Torres SK et al (2012) Biosynthesis of selenium nanoparticles by *Pantoea agglomerans* and their antioxidant activity. J Nanopart Res 14:1–9. https://doi.org/10.1007/s11051-012-1236-3
Tran PA, Webster TJ (2011) Selenium nanoparticles inhibit *Staphylococcus aureus* growth. Inter J Nanomed 6:1553–1558
Triantis T, Troupis A, Gkika E, Alexakos G, Boukos N, Papaconstantinou E, Hiskia A (2009) Photocatalytic synthesis of Se nanoparticles using polyoxometalates. Catal Today 144:2–6. https://doi.org/10.1016/j.cattod.2008.12.028
Udayalaxmi G, Himabindu D, Ramadass G (2010) Geochemical evaluation of groundwater quality in selected areas of Hyderabad, A.P, India. Ind J Sci Technol 3:546–553
Van Overschelde O, Guisbiers G, Snyders R (2013) Green synthesis of selenium nanoparticles by excimer pulsed laser ablation in water. APL Mater 1:042114–042117
Venkateswara Rao B, Kavitha C, Murthy NN, Lakshminarayana P (2016) Heavy metal contamination of groundwater in Nacharam industrial area, Hyderabad, India. J Indian Geophys Union 20:171–177
Wang Q, Webster TJ (2013) Inhibiting biofilm formation on paper towels through the use of selenium nanoparticles coatings. Inter J Nanomed 8:407–411
Wang T, Yang L, Zhang B, Liu J (2010) Extracellular biosynthesis and transformation of selenium nanoparticles and application in H_2O_2 biosensor. Colloid Surf B 80:94–102. https://doi.org/10.1016/j.colsurfb.2010.05.041
Wang Y, Yan X, Fu L (2013) Effect of selenium nanoparticles with different sizes in primary cultured intestinal epithelial cells of crucian carp, *Carassius auratus gibelio*. Inter J Nanomed 8:4007–4013
Wang J, Zhang Y, Yuan Y, Yue T (2014) Immunomodulatory of selenium nanoparticles decorated by sulfated *Ganoderma lucidum* polysaccharides. Food Chem Toxicol 68:183–189. https://doi.org/10.1016/j.fct.2014.03.003
Yang LB, Shen YH, Xie AJ, Liang JJ, Zhang BC (2008) Synthesis of Se nanoparticles by using TSA ion and its photocatalytic application for decolorization of cango red under UV irradiation. Mater Res Bull 43:572–582. https://doi.org/10.1016/j.materresbull.2007.04.012
Zhang W, Chen Z, Liu H, Zhang L, Gao P, Li D (2011) Biosynthesis and structural characteristics of selenium nanoparticles by *Pseudomonas alcaliphila*. Colloid Surf B 88:196–201. https://doi.org/10.1016/j.colsurfb.2011.06.031
Zheng S et al (2014) Selenite reduction by the obligate aerobic bacterium *Comamonas testosteroni* S44 isolated from a metal-contaminated soil. BMC Microbiol 14:204. https://doi.org/10.1186/s12866-014-0204-8